RESEARCH

Low-magnitude seismic swarms in the Calabrian Arc (Italy)

Giuseppe Davide Chiappetta ·
Mario La Rocca

Abstract Seismic swarms of low magnitude earthquakes occur frequently in the Calabrian Arc. During the last few years, several earthquakes of magnitude up to $M_L 4.4$ occurred both on land and offshore near the coast of Calabria. Some of them were followed by a sequence of tens to hundreds of smaller, well-clustered earthquakes that occurred during the following weeks or months. In other cases, swarms of low-magnitude earthquakes occur without a classical mainshock-aftershock evolution. In this work, we selected swarms that were well recorded by a high number of seismic stations to perform a detailed analysis consisting of the determination of the relative location and focal mechanism for as many earthquakes as possible. In some cases, the relative location allows to recognize the seismogenic fault and to distinguish the fault plane from the auxiliary plane of the focal mechanism solution. In other cases, the relative location unravels a small cloud of events that is not compatible with a unique fault plane, suggesting the occurrence of the swarm in highly fractured seismogenic volume. The relative hypocenter positions allow to estimate the size of the seismogenic volume, which is very small in most of the cases, often less than 1 km³. However, its extension is greater than the size computed for the mainshock rupture in many cases. The most common source mechanism is of normal type, but strike-slip and reverse kinematics are also found, in particular for swarms located offshore and near the coast. The temporal distribution of events does not show any evident migration of the sources, thus suggesting that the driving mechanism is not related with aseismic phenomena like fluid diffusion and stress waves.

Keywords Seismic swarm · Focal mechanism · Relative location · Source volume · Stress field

1 Introduction

The occurrence of sequences and swarms of small- to medium-size earthquakes has been observed globally in many regions. This type of seismicity is rather common in volcanic environments, where the driving mechanism is related to fluid migration (McNutt 2005). Moreover, swarms of small- to medium-sized events constitute part of the natural background seismicity in a tectonic environment, and sometimes, it can be artificially induced by activities related to oil and gas and geothermal energy extraction (Ellsworth 2013). In many cases, volcanic swarms and induced seismicity are monitored and studied with great detail

G. D. Chiappetta
Istituto Nazionale di Oceanografia e di Geofisica
Sperimentale, Via Treviso, 55, 33100 Udine, CS, Italy

Present Address:
G. D. Chiappetta (✉) · M. La Rocca
Università della Calabria, Via P. Bucci, 12B, 87036 Rende, CS, Italy
e-mail: gchiappetta@ogs.it

thanks to the presence of ad hoc, high-performance monitoring networks. On the contrary, most of natural swarms in a tectonic environment suffers a poorer coverage as their study relies only of regional seismic networks that often are quite sparse. However, a detailed monitoring and analysis of small earthquake tectonic swarms may give important insights about the features of active seismogenic sources, with benefits for the estimation of seismic hazard. Examples of detailed analysis of low-magnitude swarms are described by many authors (Deichmann and Garcia-Fernandez 1992; Jenatton et al. 2007; Carmona et al. 2009; Barani et al. 2014; Van Noten et al. 2015; Hauksson et al. 2016, 2017; Calderoni et al. 2021; Totaro et al. 2015; Thouvenot et al. 2016; Suarez et al. 2016; Pastori et al. 2021, and many others).

Calabria is considered one of the regions with the highest seismic hazard in Italy, mostly due to the many strong earthquakes that struck the area in the past centuries (https://emidius.mi.ingv.it/CPTI15-DBMI15/, http://storing.ingv.it/cfti/cfti5/). In fact, at least six earthquakes have been classified as XI MCS degree, which occurred in 1638, three in 1783, in 1905, and in 1908 (Rovida et al. 2020, 2022; Pino et al. 2009; Tertulliani and Cucci 2009). Some active seismogenic sources are inferred from the location of past earthquakes and from the surface morphology (https://diss.ingv.it/diss330/dissmap.html, http://sgi.isprambiente.it/ithaca/viewer/index.html), while other active faults remain debated due to the lack of instrumental seismicity (https://diss.ingv.it/diss330/dissmap.html). During the last 50 years, the seismicity of the Calabrian Arc has been rather low, consisting of events with M ≤ 5. The lack of M > 5 earthquakes and a rather sparse monitoring network in the past decades (Michelini et al. 2016) hampers a precise identification and characterization of the active seismogenic sources.

In this work, we analyze a subset of the crustal seismicity that occurred in the Calabrian Arc during the last 10 years. Here, several swarms of small- to medium-sized earthquakes occurred in many parts of the region. Since small earthquakes are more abundant than larger events, the comprehensive study of their source may be one of the keys to understand and forecast the features of stronger events. For this reason, detailed analysis of seismic swarms and low-magnitude earthquakes is gaining an increasing attention in recent years (Chen and Shearer 2011; Hauksson et al. 2016, 2017; Brodsky 2019; Ross et al. 2019; Passarelli et al. 2018; Napolitano et al. 2020).

We performed detailed analyses on swarms recorded by a high number of seismic stations in order to compute the relative location of the hypocenters and the focal mechanism of as many events as possible. The relative location of well clustered sources may provide an important constraint on the fault position, extension, and geometry, also allowing for the characterization of the seismogenic volume that produced the swarm. The relative location of small- to medium-sized earthquakes is a consolidated processing tool in seismology, as testified by a number of successfully applications during the last decades. Many authors have applied relative location techniques to earthquake clusters, showing how the cloud of absolute independent locations usually shrinks to much smaller volumes that sometimes depict a fault geometry (Ito 1985; Deichmann and Garcia-Fernandez 1992; Scherbaum and Wendler 1986; Stich et al. 2001; Shearer et al. 2003; Vidale and Shearer 2006; Carmona et al. 2009; Napolitano et al. 2021). Following the determination of the relative location, we estimated the extension of the seismogenic volume of the considered swarms; then, we made a comparative analysis with the size of the mainshock rupture. In fact, in other regions, this analysis has shown that often the extension of the volume occupied by the swarm is considerably greater than that expected from the mainshock rupture size (Passarelli et al. 2018; Roland and McGuire 2009; Vidale and Shearer 2006). Finally, we aim to obtain more insights on the seismogenic sources and the stress field, in order to obtain information that can be beneficial for a more accurate assessment of the local seismic hazard.

2 Swarms and sequences

A seismic swarm consists of a sequence of earthquakes located in a reasonably small crustal volume, occurring irregularly in time and without a clear mainshock-aftershock order (Van Noten et al. 2015). On the other hand, a swarm that begins with a strong event that can be considered the mainshock, followed by a series of events of lower magnitude, is usually called a seismic sequence. In this work, such a distinction will not be strictly applied because some cases are rather ambiguous (e.g., the sequence is triggered by a mainshock, but it is part of an ongoing swarm (Guerra et al. 2005; Vidale and Shearer 2006; Totaro et al. 2013; Napolitano et al. 2021; De Gori et al. 2022). Swarms and sequences occur frequently

in the Calabrian Arc, but only a few have been analyzed in detail (Giampiccolo et al. 2008; Guerra et al. 2005; Totaro et al. 2013, 2015; Napolitano et al. 2020, 2021; Calderoni et al. 2021; De Gori et al. 2022) due to the not ideal configuration of the monitoring seismic network until a few years ago. Considering the number of earthquakes and the cumulative released energy, the most important seismic swarm occurred at Mt. Pollino from 2010 to 2014, being composed by thousands of earthquakes of magnitude up to $M_L 5.0$ (Totaro et al. 2015; Napolitano et al. 2018, 2020, 2021; Pastori et al. 2021; De Gori et al. 2022). This swarm has been analyzed in detail by several authors (Totaro et al. 2013; 2015; Napolitano et al. 2020, 2021; Pastori et al. 2021), and in this work, we do not consider it for our analysis. However, we will use some published results for a quantitative comparison with the swarms analyzed here.

In this work, we performed detailed analysis only for swarms occurred during the last few years and recorded by a sufficient number of seismic stations within about 40 km from the epicenter. Swarms composed by many earthquakes without a mainshock-aftershock order have been identified in the following places: offshore Crotone (more than 50 events in 2020, Mmax 4.0), Bocca di Piazza (120 events in 2014, Mmax 4.0), and Rocca di Neto (100 events in 2013, Mmax 2.8). In some places, small earthquakes are numerous but diluted during many years, like Caraffa di Catanzaro (200 events in 10 years, Mmax 4.0), Bocca di Piazza (more than 400 events in 10 years, Mmax 4.0), Serralonga (140 events, Mmax 3.1), and Cicala (many swarms with tens of events through the years, Mmax 3.3). Notable examples of sequences triggered by a mainshock occurred at Albi (130 events in 2020, Mmax 3.8), offshore Amantea (60 events, mostly in 2020, Mmax 3.9), Punta Alice (150 events in 2020, Mmax 3.2), San Pietro di Caridà (Mesima valley, 150 events in 2019, Mmax 3.6), Aspromonte (90 events in 2020, Mmax 2.7), offshore Bagnara Calabra (140 events in 2018, Mmax 4.0), Alessandria del Carretto (60 events in 2017, Mmax 2.6), and Catanzaro Lido (36 events in 2022, Mmax 4.3). Figure 1 shows the epicentral area of the identified swarms: in red those analyzed in this work and in gray those not analyzed because available data are not adequate for detailed analyses. The same figure shows also the seismic stations currently installed in the region.

3 Data analysis

For each analyzed earthquake, the first step of our procedure was the manual picking of P and S waves on all available recordings. The source location was performed through the software HYPOSAT (Schweitzer 2001, 2006) using a 1D velocity model (Table 1). Table 2 resumes the results of absolute location for the swarms analyzed in this work, including the average location errors, the average location gap, and the depth range. For each swarm, we chose a reference earthquake and computed the relative location of other events with respect to the reference, assuming that azimuth ϕ and takeoff θ angles can be considered the same at a given seismic station. This assumption works very well if the distance between the two hypocenters is much smaller than the hypocenter-station distance. The computation of relative location further requires the estimation of the travel time difference Δt at each site for any earthquake pairs. Then, the relative hypocenter coordinates (Δx, Δy, Δz, ΔT_0) are estimated by solving the system of N equations:

$$\frac{1}{v}\begin{pmatrix} \sin\theta_1\sin\phi_1 & \sin\theta_1\cos\phi_1 & -\cos\theta_1 & v \\ \sin\theta_2\sin\phi_2 & \sin\theta_2\cos\phi_2 & -\cos\theta_1 & v \\ \vdots & \vdots & \vdots & \vdots \\ \sin\theta_N\sin\theta_N & \sin\theta_N\cos\phi_N & -\cos\theta_N & v \end{pmatrix}\begin{pmatrix} \Delta x \\ \Delta y \\ \Delta z \\ \Delta T_0 \end{pmatrix} = \begin{pmatrix} \Delta t_1 \\ \Delta t_2 \\ \vdots \\ \Delta t_N \end{pmatrix}$$

$$(1)$$

where and ϕ_k, θ_k, and Δt_k are the azimuth, takeoff, and delay time at the kth seismic station, respectively. This mathematical problem is easily solved with matrix methods obtaining the relative coordinates between the two hypocenters (Menke 1984). This method is the same proposed by Got et al (1994), but without the restriction of similar waveform among the analyzed events. We do not limit the analysis to events with similar waveform because we want to keep as many events as possible in our relative location. We estimate the time delay through the most careful possible picking of the P wave onset performed on seismograms oversampled at 200 sps and high pass filtered (2 Hz, causal filter, to improve the signal-to-noise ratio). As expected, the hypocenters obtained from the relative location are distributed in a smaller volume compared with the results of absolute location. Solving Eq. (1) provides also the residual on the time differences, from which the uncertainty on the relative location can be easily computed.

The 3D distribution of relative hypocenters was evaluated finding the best-fitting plane possibly

Fig. 1 Epicentral area of seismic swarms analyzed in this work (red circle) and of swarms analyzed in previously published papers (yellow circle). Gray circles represent swarms occurred in recent years but recorded by few seismic stations for the analyses performed in this work. Triangles represent the seismic stations available at present in the Calabrian Arc
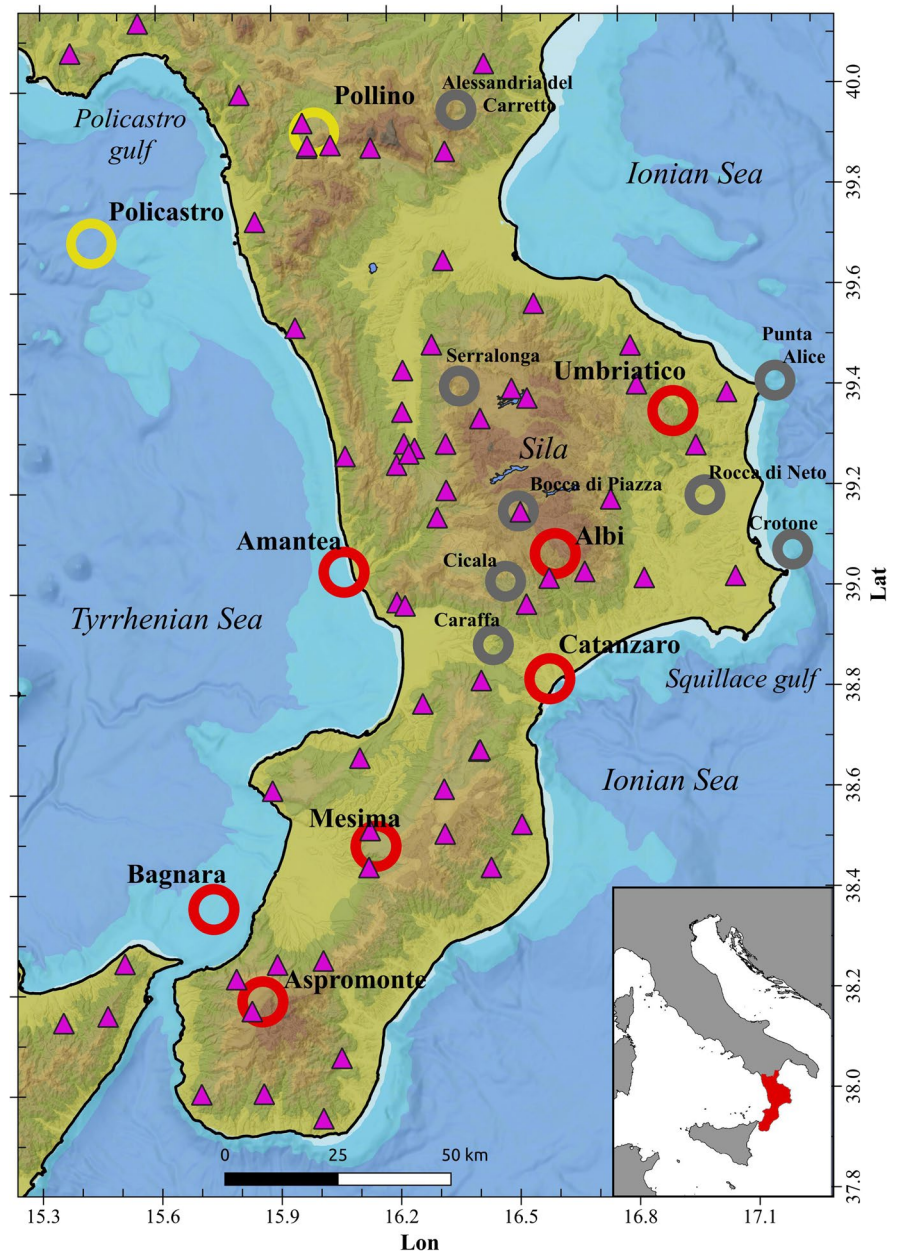
corresponding to a unique fault causing the events in the swarm. With this aim the 3D points cloud was interpolated by the equation $Z = aX + bY + c$, which analytically describes a plane. The uncertainty on the two parameters a and b gives an idea about the fit goodness. From a and b, we compute strike and dip of the best fit plane, according to the following relations:

$$strike = \arctan\left(-\frac{b}{a}\right) \quad dip = \arctan\left(\sqrt{a^2 + b^2}\right)$$

The strike is possibly increased by 180 degrees to have values in the range 0–360°, in accordance with the standard convention. Strike and dip obtained through this procedure are compared with those found from the computation of focal mechanisms, as described below. Successful applications of this technique to multiple earthquakes are described in several papers (e.g., Shearer et al. 2003; Carmona et al. 2009; Napolitano et al. 2021, and references therein).

Table 1 Velocity model used for earthquake location

Z (km)	V_p (km)	V_s (km)
− 1.0	4.00	2.286
0.67	4.42	2.552
2.67	4.69	2.708
4.67	5.23	3.020
6.67	6.00	3.464
12.34	6.12	3.533
18.34	6.38	3.684
30.00	7.69	4.440
36.67	7.70	4.446
43.34	7.73	4.463
60.0	8.10	4.620

The Matlab functions *boundary* and *alphaShape* were used to compute the volume (*V*) and the surface area (*A*) of the polyhedron enveloping the hypocenters obtained from the relative location. Since our aim is to estimate the volume of the swarm source, which is a volume that contains all individual sources of the swarm earthquakes, we computed an additional volume to consider the spatial extension of real sources. We considered each earthquake source as a sphere of radius *r*, centered at the corresponding hypocenter; then, the surface of the polyhedron that contains all hypocenters is multiplied by *r* to estimate an additional volume that considers a radius of *r* km around each hypocenter. Assuming $r = 0.1$ km, which is a reasonable source radius for $2.0 < M_L < 2.5$ earthquakes,

we computed the final volume *SV* through the relation: $SV = V + rA$. The sum of the polyhedron volume and the additional surface thickness gives an estimation of the seismogenic volume that likely contains all located sources of the swarm, including their extension. The value $r = 0.1$ km is greater than the error associated with the relative location (Table 3); thus, the volume estimated through this procedure includes also the location error. A graphical example of the volume computed for the swarm occurred near Albi is shown in Fig. 2e. Since most earthquakes of each swarm are smaller than $M_L 2$, it follows that the computed volume is likely an overestimation of the true seismogenic volume. For each swarm, we compare the size of the seismogenic source with the size of the mainshock rupture derived from the magnitude, assuming a circular fault with uniform dislocation (Table 3).

Regarding the computation of the focal mechanism, since the majority of events have magnitude lower than 3, we could only rely on the analysis of polarity and amplitude of direct waves, using the FOCMEC (Snoke et al. 1984) and HybridMT (Kwiatek et al. 2016) codes. FOCMEC searches for fault plane solutions that satisfy the polarity of P wave and possibly of SV and SH wave, given azimuth and takeoff angles. HybridMT searches for moment tensor solutions that satisfy the P wave polarity and amplitude, estimated from the area below the first pulse of the ground displacement signal. The reliability of the solutions given by these two methods

Table 2 Seismic swarms analyzed in this work. Results of absolute location

Swarm name	Mmax	Starting no. of EQ [mag range]	Source depth range	Average location gap (degrees)	D_lat (km)	D_lon (km)	D_z (km)	Min. epicenter — station distance (km)
Albi	3.8	128 [0.6–3.8]	7–12	95	1.08	0.93	2.28	5.1
Amantea	3.9	55 [0.7–3.9]	20–24	188	0.70	1.49	1.53	14.6
Aspromonte	2.7	97 [0.5–2.7]	5.7–7.2	94	0.72	0.84	1.40	3.3
Bagnara Calabra	4.0	98 [0.6–4]	16–22	134	1.12	1.15	2.78	19.1
Catanzaro	4.3	41 [1–4.3]	35–40	141	2.77	4.86	4.45	13.8
Mesima	3.6	172 [0.7–3.6]	16–19	97	0.43	0.40	0.91	3.8
Umbriatico	3.3	85 [1–3.3]	25–28	122	1.18	1.59	2.09	9.0
Policastro[1]	4.4	>120	8–16	>200	1.45	2.05	5.5	32 to 40
Pollino[2]	5.0	401	4.1–6.5	80	1.78	1.65	2.8	<1

[1]Results from Calderoni et al. (2021)

[2]Results from Napolitano et al. (2021)

Table 3 Seismic swarms analyzed in this work. Relative location

Swarm name	Mmax	Starting no. of EQ	No. of events rel location [mag range]	Average rel loc error (m)	SV (km³)	Swarm source radius (km)	Mainshock source radius (km)	No. of focal mechanism [mag range]
Albi	3.8	128	96 [0.9–3.8]	51	6.3	2.8	0.42–0.65	8 [1.6–3.8]
Amantea	3.9	55	31 [0.7–3.9]	17	2.3	3	0.47–0.72	3 [2.5–3.9]
Aspromonte	2.7	97	54 [0.7–2.7]	39	0.3	0.7	0.13–0.20	1 [2.7]
Bagnara Calabra	4.0	98	37 [1.2–4]	85	1.1	1.2	0.53–0.81	4 [3.1–4.0]
Catanzaro	4.3	41	23 [1.1–4.3]	70	5.4	1.4	0.72–1.12	2 [3–4]
Mesima	3.6	172	55 [1.6–3.6]	55	0.6	0.8	0.34–0.52	7 [2.4–3.6]
Umbriatico	3.3	85	40 [1–3.3]	53	1.2	1.2	0.25–0.38	3 [2.3–3.3]
Policastro[1]	4.4	>120	28 [2.4–4.4]	-	23	6	0.81–1.24	8 [2.9–4.4]
Pollino[2]	5.0	401	401 [0.6–2.7]	-	2.76	4	(M5: 1.54–2.38)	17 [1.0–2.7]

[1]Results from Calderoni et al. (2021)
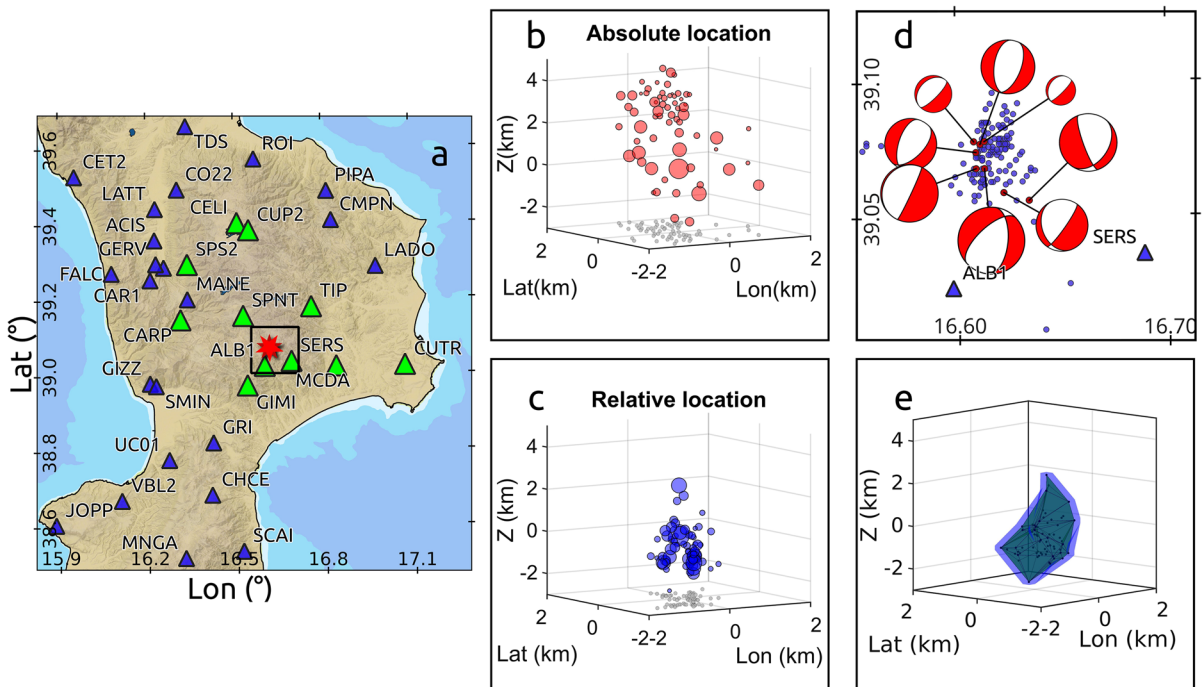
[2]Results from Napolitano et al. (2021)

Fig. 2 a Epicentral area of Albi swarm and seismic stations used in this work. Green triangles show the stations used for the relative location. **b** 3D view of the absolute and **c** relative located hypocenters. **d** Focal mechanism of the strongest events of the swarm. **e** 3D view of the seismogenic volume

is as more reliable as better the focal sphere is sampled by earthquake recordings. The uneven azimuthal coverage of the seismic source often makes unreliable the results of focal mechanism analysis, particularly for very small earthquakes for which the first pulse

polarity is clear only at short distances. Therefore, for some swarms, we could obtain a reliable focal mechanism solution for earthquakes as small as $M_L 1.6$, while for other swarms, determining the kinematics of events smaller than $M_L 2.5$ was impossible.

However, it is important to point out that for earthquakes of magnitude $M_L < 3$, the methods based on the first pulse features are the only possibility we have to investigate the source kinematics because for such small events the methods based on the comparison between real and synthetic signals fail. Both software, FOCMEC and HybridMT, revealed to be very efficient for the analysis of small earthquakes carried out in this work, and they gave always similar results. For the few earthquakes of magnitude $M_L > 3.5$, the focal mechanism was computed also with the software gCAP (Zhu and Ben-Zion 2013), which compares observed and synthetic signals. In any cases, the result is the same or very similar to those provided by FOCMEC and HybridMT.

4 Results

A preliminary selection of many swarms was made analyzing the catalog of the crustal seismicity in the last decade available online at http://terremoti.ingv.it/. We identified seven swarms appropriate for our analysis, as resumed in Tables 2 and 3. In four cases, the station distribution was very favorable (Albi, Mesima, Aspromonte, Umbriatico), while in three other cases, the azimuthal gap is rather high (Amantea, Bagnara, Catanzaro, $130 < gap < 190$).

One of the better covered swarms occurred near the village of Albi (Fig. 2) in 2020. Its events were recorded by 12 seismic stations at distance smaller than 40 km and with an azimuthal gap of about 95° (Fig. 2). Using the location of the mainshock (M_L 3.8, event 20200116 233709), we selected about 130 earthquakes occurred in 2020 and located within 10 km from the epicenter. All these events were relocated after an accurate phase picking; then, we excluded those events having less than 11 phase picks and with a distance from the mainshock hypocenter larger than 4 km. This selection excluded the smallest events leading to a total of 96 earthquakes with magnitude in the range $0.9 \leq M_L \leq 3.8$ (Table 3). The relative location of these events shows a source volume elongated in the vertical direction, without a clear planar arrangement geometry that could suggest a unique fault surface. The hypocenter distributions obtained from the absolute and relative locations are shown in Fig. 2b and c, respectively. The seismogenic volume estimated for this swarm is 6.3 km³, centered at 10.2

km depth (Fig. 2e; Table 3). The length of this volume in the vertical direction is of about 5 km, which is much larger than the source radius of the mainshock, expected to be in the range 0.42–0.65 km. For the Albi swarm, we obtained a reliable focal mechanism for 8 events in the magnitude range 1.6–3.8 (Tables 3 and 4). All of them are of normal type, but with some differences in the strike direction, and an oblique component in many cases (Fig. 2d). The average kinematics of the swarm is given by strike = 34°, dip = 58° and rake = −79° (Table 5). The different focal mechanisms (Table 4) and scattered hypocenters explain the large variety of waveforms that are observed at the same site for different events of this swarm, as shown in Fig. 3a for the 15 strongest events.

The Mesima valley swarm of 2019 was well recorded by 12 seismic stations at distances within 40 km from the epicenter (Fig. 1). The mainshock was M_L 3.6, and the most of the following events had small magnitude, but the ideal station distribution and high quality of the recorded data allowed for a reliable absolute and relative solution of the hypocenter location for events as small as M_L 1.6. We started with a selection of 172 events and could retain 55 of them for the relative location (Tables 2 and 3). In this case, the relative hypocenter distribution has a flat shape that is well fitted by a plane (Fig. 4a), suggesting that the Mesima swarm was likely generated by a unique fault patch at ~17.5 km depth, with strike = 59° and dip = 58°. The seismogenic volume computed in this case is only 0.6 km³, a value ten times smaller than the case of Albi swarm (Table 3). For the Mesima swarm, the size of the hypocenter distribution is about twice the size of the mainshock rupture. This result suggests that most events of the swarm occurred on the same small fault patch, and aftershocks were likely triggered by the stress field change around the mainshock rupture. The focal mechanism was determined for 7 events of the Mesima swarm which all showed a normal kinematics (Fig. 5a). The predominant mechanism has strike = 54° and dip = 46°, in good agreement with the fault plane found from the fit of the hypocenter distribution (Table 5). Seismograms of the events of Mesima valley swarm are characterized by higher similarity compared with Albi swarm (Fig. 3b), as expected from earthquakes occurring on the same fault, and with highly similar kinematics.

The swarm of Umbriatico, which occurred in 2022, consists of two main events of similar magnitude,

Table 4 Results of focal mechanism analysis

Swarm/Earthquake	Lat	Lon	Depth	Mag	Strike	Dip	Rake	Strike	Dip	Rake
Albi					Focmec			HybridMT		
20200116233709	39.068	16.613	10.2	3.8	6	45	−121	20	58	−89
20200120050639	39.077	16.611	9.3	2.9	22	47	−80	24	31	−71
20200123054238	39.074	16.609	7.9	2.8	45	45	−70	37	74	−82
20200130153154	39.059	16.622	9.7	2.8	35	78	−73	38	78	−78
20200202192408	39.056	16.634	12.0	3.1	35	26	−38	34	64	−70
20200208225904	39.068	16.609	7.0	3.1	25	85	−90	44	82	−89
20200229170550	39.078	16.608	6.9	2.0	45	70	−90	14	78	−99
20200320173243	39.078	16.613	6.9	1.6	45	75	−85	45	70	−55
Amantea	Lat	Lon	Depth	Mag	Strike	Dip	Rake	Strike	Dip	Rake
20200317004719	39.032	16.080	24.6	2.5	185	89	−159	350	39	157
20200317005255	39.034	16.054	24.4	3.9	262	75	9	327	26	130
20200428200246	39.035	16.059	24.0	2.9	252	73	−15	244	63	−19
Aspromonte	Lat	Lon	Depth	Mag	Strike	Dip	Rake	Strike	Dip	Rake
20201024223426	38.187	15.858	7.1	2.7	6	25	−78	3	54	−71
Bagnara	Lat	Lon	Depth	Mag	Strike	Dip	Rake	Strike	Dip	Rake
20180928052431	38.375	15.731	18.5	4.0	245	72	−98	256	77	−91
20180928120357	38.362	15.727	17.3	3.2	271	50	−96			
20181003012301	38.376	15.724	18.2	3.1	255	50	−80	251	82	−93
20181114150102	38.376	15.736	17.2	3.4	259	59	−109	241	69	−97
Catanzaro Lido	Lat	Lon	Depth	Mag	Strike	Dip	Rake	Strike	Dip	Rake
20221012224455	38.822	16.571	36.4	4.4				32	48	87
20221018031028	38.831	16.584	36.6	3.0				102	66	135
Mesima					Focmec			HybridMT		
20190526233157	38.494	16.144	19.1	3.6	73	43	−82	45	49	−75
20190527112715	38.492	16.145	17.6	2.9	85	53	−71	58	48	−76
20190601091419	38.493	16.146	19.1	3.4	37	45	−104	38	50	−75
20190609192200	38.495	16.148	19.4	2.4	79	43	−79			
20190620091558	38.495	16.148	20.8	3.3	24	61	−78			
20190620212422	38.495	16.145	19.0	3.0	56	43	−93			
20190623001611	38.498	16.148	18.1	2.5	34	34	−100			
Umbriatico					Focmec			HybridMT		
20220519210108	39.358	16.903	26.0	3.2	280	49	−24	319	44	−4
20220519210653	39.363	16.904	23.8	2.3	302	41	−36	310	45	−12
20220520035919	39.354	16.91	25.3	3.3	312	25	72	336	27	90

$M_L 3.2$ and $M_L 3.3$, which occurred a few hours apart, and many tens of smaller earthquakes, all located at depth between 25 and 28 km. The majority of events occurred during the first two days (Fig. 6c). The relative locations of 40 events unravel a planar geometry striking 299° and dipping 63° (Fig. 4b). The computed seismogenic volume is 1.2 km^3. We obtained a reliable focal mechanism only for the three most energetic events ($M_L 3.3$, $M_L 3.2$, $M_L 2.3$), showing dissimilar result, being one event with reverse mechanism while

the other two with oblique strike slip (Fig. 5b). However, the direction of the P axis for these earthquakes is very similar, nearly horizontal and E-W oriented, indicating a compressive stress field in the E-W direction. This result suggests that the two main events occurred on two different faults near their intersection. This local stress field is compatible with the focal mechanism of earthquakes that occur in the NE sector of Sila massif (Presti et al. 2013; Orecchio et al. 2021; Frepoli and Amato 2000).

Table 5 Comparison between strike and dip from the hypocenters fit and from focal mechanism analysis

Swarm	Plane fitting hypocenters		Predominant kinematics		
	Strike fit	Dip fit	Strike	Dip	Rake
Albi	-	-	34	58	− 79
Amantea	-	-	263	88	1
Aspromonte	358	49	6	25	− 78
Bagnara Calabra	-	-	261	64	− 93
Catanzaro	243	58	-	-	−
Mesima	59	58	54	46	− 86
Umbriatico	299	63	-	-	−
Pollino	151	49	143	48	− 106
Policastro	-	-	67	79	− 8

A swarm of about 100 small earthquakes occurred in Aspromonte massif in 2020. Among 97 selected events, 54 were appropriate for the relative location. All events had small magnitude ($M_L \leq 2.7$; Tables 2 and 3) and occurred at shallow depth, between 5.7 and 7.2 km. The hypocenter distribution is almost planar (Fig. 4c), and the estimated seismogenic volume is only 0.3 km^3. The very low magnitude of these earthquakes did not allow for a reliable estimation of the focal mechanism other than the mainshock, which shows a normal kinematics (Fig. 5c).

Amantea swarm is located offshore (Figs. 1 and 5d) close to the western coast of Calabria, characterized by mainshock of magnitude $M_L 3.9$ and depth between 20 and 24 km. In spite of the high
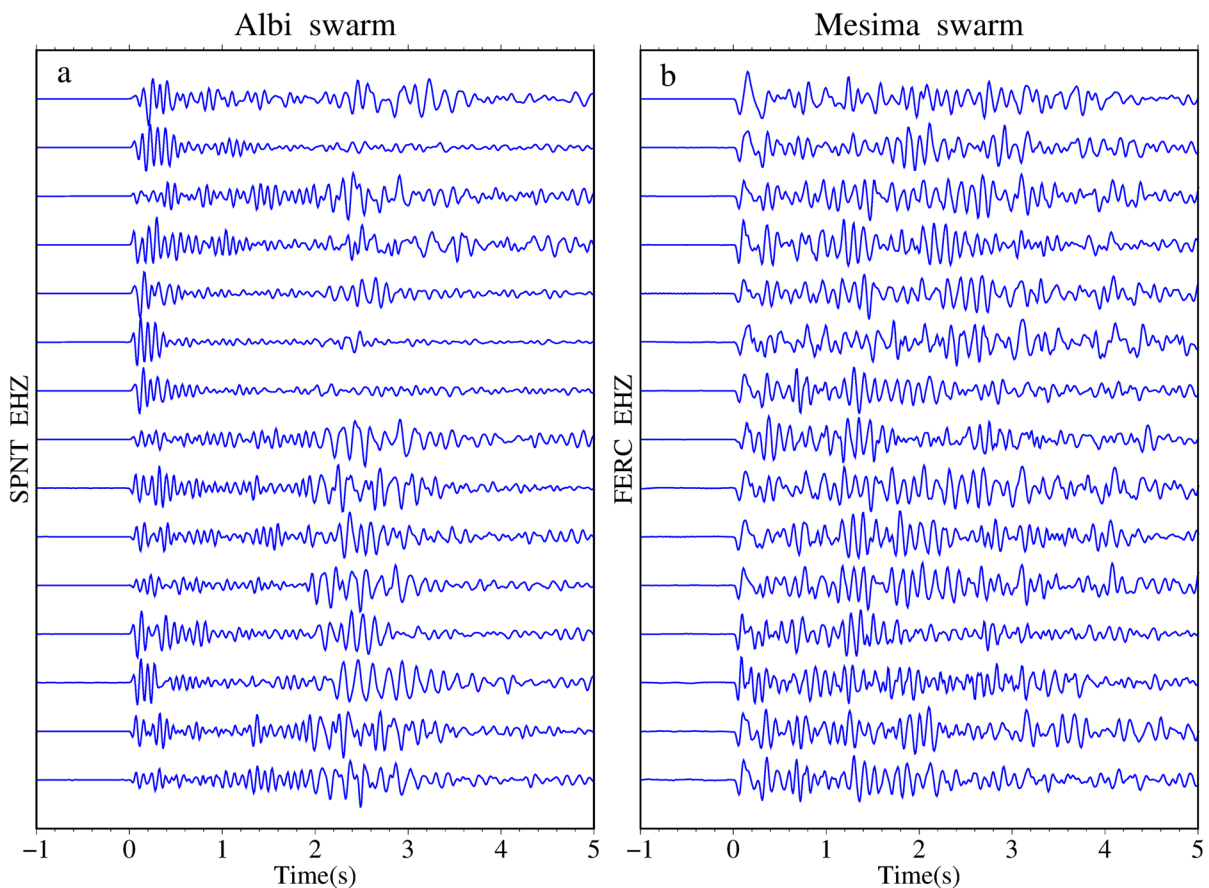
Fig. 3 (Left) Seismograms of the Albi swarm as recorded by the vertical component of SPNT station. (Right) Seismograms of the Mesima swarm recorded by the vertical component of FERC seismic station
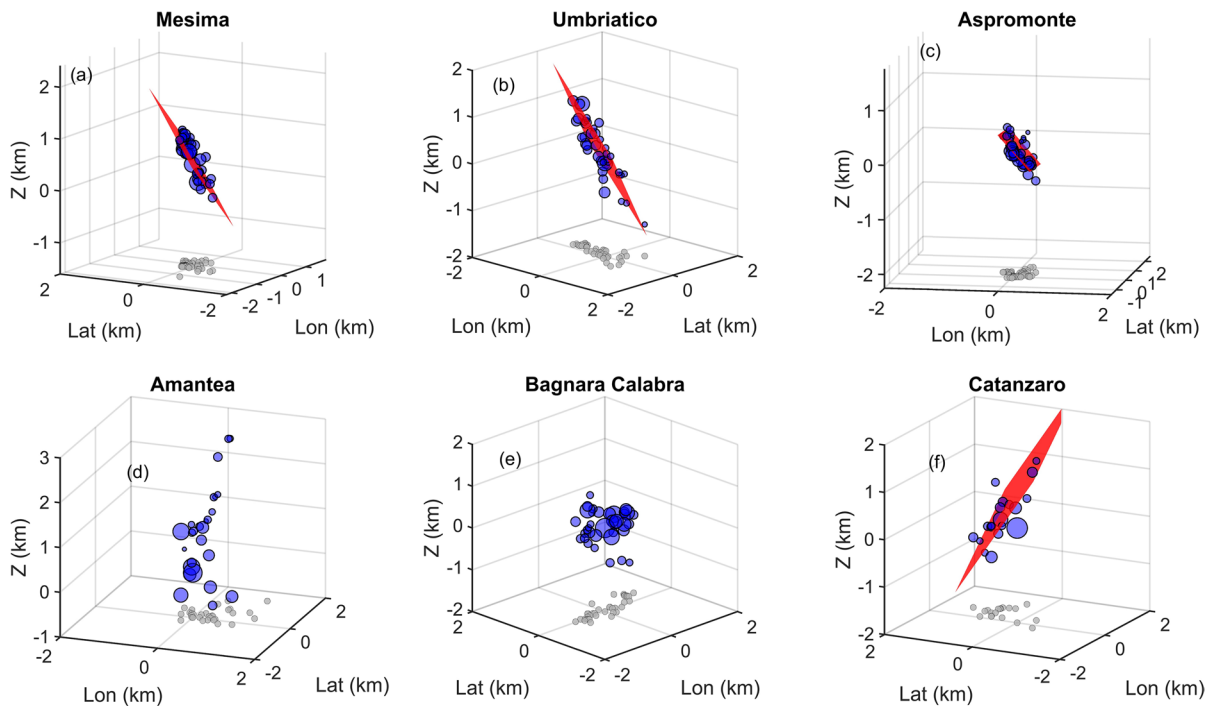
Fig. 4 3D view of the relative located hypocenters of six swarms

azimuthal gap of the recording stations (Fig. 1; Table 2), we obtained a good relative location for 31 earthquakes in the magnitude range 0.7–3.9, with a seismogenic volume of 2.3 km³ (Table 3). The relative hypocenter distribution is vertically elongated even though no clear planar distribution could be inferred (Fig. 4d). The three computed focal mechanisms are very similar among them, with strike slip kinematics (Table 4; Fig. 5d).

The swarm of Bagnara Calabra occurred about 15 km offshore in 2018 (Fig. 1), with a maximum magnitude M_L4.0 and about 100 earthquakes at depth between 16 and 22 km. The relative location of 37 events gives a volume of 1.1 km³. The hypocenter distribution is elongated in the E-W direction but without a planar shape (Fig. 5e). The focal mechanisms computed for the four strongest events are characterized by normal kinematics with E-W strike (Table 4; Fig. 5e).

A swarm of more than 40 events was triggered by a M_L4.3 earthquake near the coast of Catanzaro in October 2022. The depth range of these earthquakes is between 35 and 40 km, while the relative location of 23

events gives a volume of 5.4 km³. The hypocenter distribution suggests a fault plane with strike 243° and dip 58° (Fig. 4f). The few focal mechanisms show different kinematics among them, but with reverse predominant features (Fig. 5f).

From the comparison of focal mechanisms, we found that the highest similarity among individual kinematics occur for the Mesima, Amantea, and Bagnara swarms, while the lowest similarity is observed for Umbriatico and Catanzaro swarms. Albi swarm is characterized by predominant normal kinematics, with some differences among the individual solutions.

5 Discussion and conclusions

The results of our analysis show interesting features about the seismogenic volume involved in the analyzed swarms, their predominant kinematics, and the corresponding stress field. In order to improve the comparison among different swarms, results found in this work have been enriched with the results
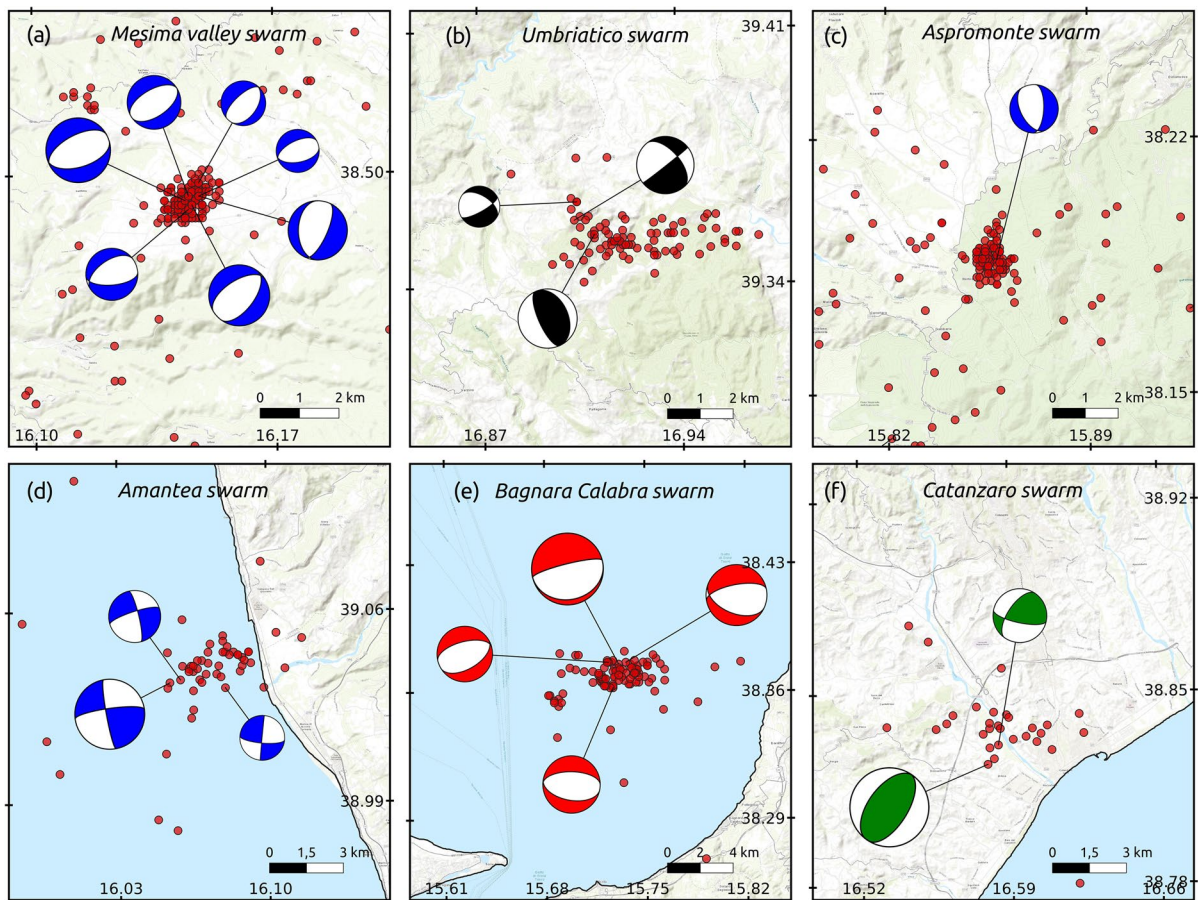
Fig. 5 Focal mechanism of the strongest and/or better recorded earthquakes of each swarm

obtained for a sequence occurred in the Policastro gulf in 2019 and part of the Pollino swarm that occurred from 2010 to 2014. Here, we use the results of relative location by Calderoni et al. (2021) and by Napolitano et al. (2021) to compute the seismogenic volume, as reported in Table 3. However, it is important to note that the relative location of these two latter swarms includes only a small subset of earthquakes, those found from the cluster analysis obtained through the cross-correlation performed to identify events with similar waveforms. The cluster analysis usually excludes many events from a swarm because their waveform does not match with others. In our work we did not apply cluster analysis in order to keep as many events as possible in our computation, thus relying only on the event magnitude (through the number of pickings) and discarding waveform similarity. For this reason, results obtained

in the present work are representative of the most energetic part of the swarm and not only of a subset of events characterized by high waveform similarity. The nine swarms resumed in Tables 2, 3, and 5 have a comparable number of events and similar maximum magnitude. However, the results obtained for the seismogenic volume span a very wide range, from 0.3 km^3 (Aspromonte swarm) to 23 km^3 (Policastro gulf). The large value for the Policastro swarm is reasonably due to the large location gap and due to the lack of any seismic stations at distance less than 40 km from the epicentral area. These conditions are unfavorable also for the relative location because they correspond to a narrow range of takeoff angle, translating into large uncertainty on the relative hypocenter depth. Excluding this result, the other swarms are still characterized by volumes in a wide range, from 0.3 to 6.3 km^3. The largest among them corresponds to the Albi

Fig. 6 Time evolution of the analyzed swarms shown as daily (blue bars) and cumulative number (orange line) of earthquakes
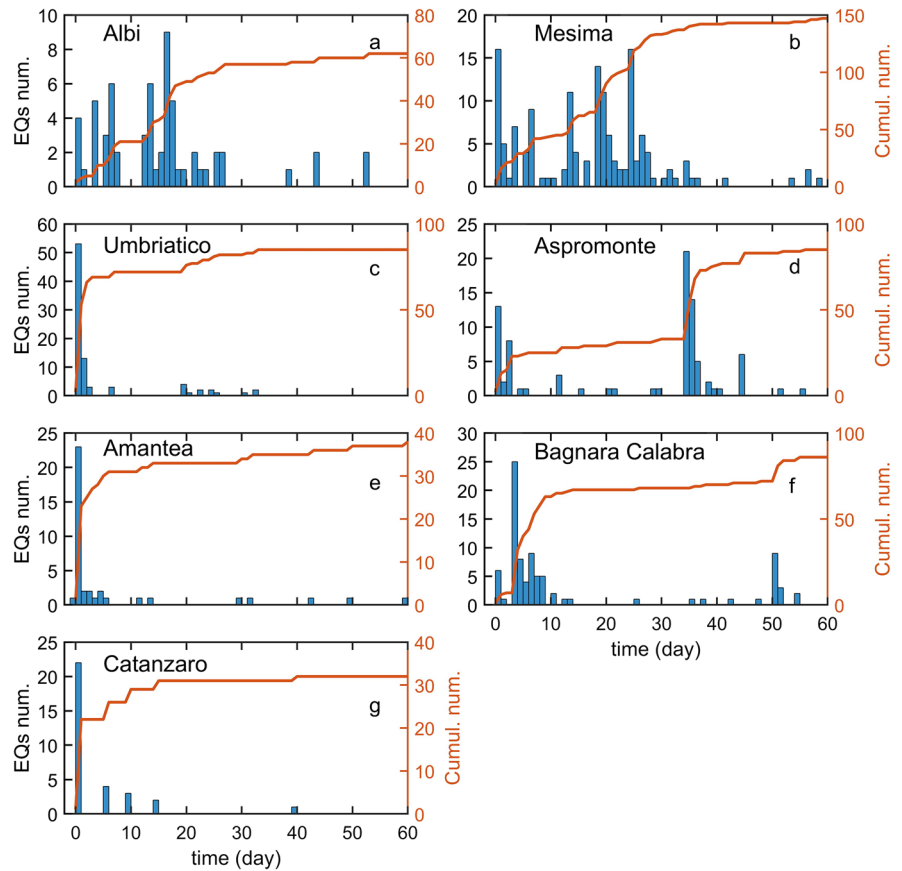
swarm, which is also ideally illuminated by many and azimuthally well distributed stations. Source volumes different by an order of magnitude found under similar conditions, like Albi, Mesima, Aspromonte, and Umbriatico swarms, mean that the difference is effective and not imputable to biased results of the relative location. Therefore, a comprehensive description of a swarm should always include the source volume among the other parameters usually given (number of events, Mmax, source location, source kinematics). This is the most interesting result of our work. The large source volume of Albi swarm, associated with the lack of any evident alignment of relocated hypocenters, indicates that the swarm was originated by a highly fractured volume under a diffuse stress field, rather than a well-defined fault patch as observed for Mesima, Aspromonte, and Umbriatico swarms. For these three latter cases, the hypocenter distribution is characterized by a narrow flat shape indicating a well-defined plane that likely represents the fault that generated all or the most of swarm localized events.

Under this hypothesis, fitting the relocated hypocenters with a plane allows to estimate strike and dip of the source fault. The comparison of strike and dip obtained from fit with strike and dip of the two planes found from the focal mechanism analysis gives the opportunity to discriminate the fault plane from the auxiliary plane in the result of focal mechanism. For such comparison, about the focal mechanism parameters, we considered the predominant kinematics of the swarm, when many individual sources have been reliably resolved, and/or the kinematics of the mainshock. This comparative analysis gives a very good result for Mesima swarm, and a sufficient agreement for Aspromonte swarm. On the contrary, for Umbriatico and Catanzaro swarms, the focal mechanisms computed for different events of the same swarm give quite different results, as shown in Fig. 5. However, it is noteworthy that also in these cases, at first sight incoherent, the various solutions are characterized by a very similar direction of the P axis. This result indicates that the driving mechanism of the swarm is

a compressive stress field acting upon a seismogenic volume characterized by many small faults with different strikes and dips. Thus, dislocations may occur on existing faults that have direction appropriate to relieve strain energy, although they are not necessarily well aligned with the maximum shear stress. This hypothesis explains the different focal mechanisms observed for earthquakes located very near to each other, as observed for Albi, Umbriatico, and Catanzaro swarms (Figs. 2 and 5).

The shallowest swarms are characterized by normal kinematics (Albi, Aspromonte, Pollino, Mesima, Bagnara), while deeper swarms show transcurrent and/or reverse mechanisms (Umbriatico, Catanzaro). The two swarms located offshore Amantea and in the Policastro gulf are characterized by strike slip kinematics. This result confirms the complexity of the active stress field in the crust of the Calabrian Arc, in agreement with previous published studies (Frepoli

and Amato 2000; Presti et al. 2013; Orecchio et al. 2021).

We computed the maximum extension of the hypocenter distribution for each swarm to compare it with the estimated size of the mainshock, computed assuming a circular fault with uniform dislocation (Table 3). For many analyzed swarms, we found a hypocenter distribution that is quite larger than the mainshock rupture size. We argue that those swarms are driven by a stress field that produces an irregular accumulation of strain energy upon a fault, or a fault system, due to heterogeneities in the involved rock volume. Then, dislocations occur on the weaker fault patches, or where accumulated strain is higher, and the strain energy is released by small earthquakes that are slightly scattered in space and time.

For each analyzed swarm, we observed carefully the timing of hypocenters to see if there is any evident migration of the sources inside the seismogenic volume (Fig. 7).

Fig. 7 Time evolution of the hypocenters of the analyzed swarms. Symbol size is proportional to magnitude while the color shows the time position in the event sequence
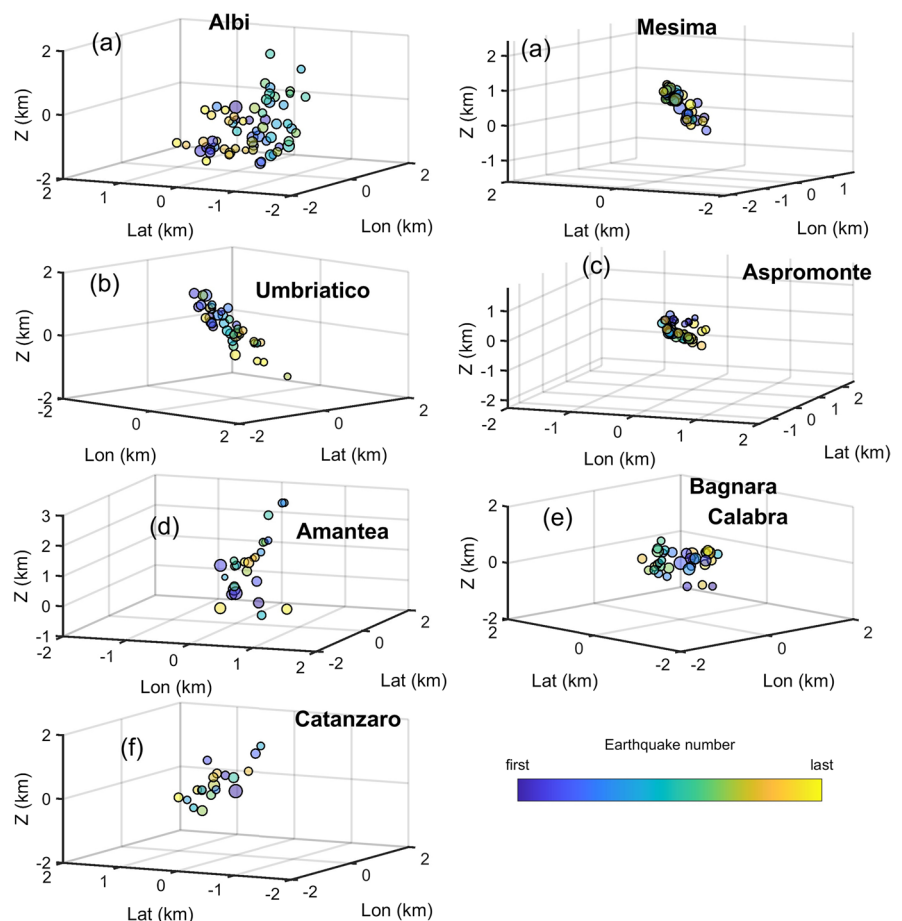
The source migration with time is an important feature of seismic swarms because it would be an important indication about possible driving mechanisms like fluid diffusion and/or stress transfer in the seismogenic volume. Several papers describe source migration during swarms and infer an important role of fluids as driving mechanism for the occurrence of many earthquakes in a small volume (Parotidis et al. 2005; Hainzl and Ogata 2005; Hainzl et al. 2012; Chen et al. 2012; Grasso et al. 2021; Ross and Cochran 2021). The important role of fluids as driving mechanism has been recognized in many cases of induced seismicity swarms (Ellsworth 2013; Parotidis et al. 2005; Eyre et al. 2019; Grasso et al. 2021), and in other tectonic swarms (Lohman and McGuire 2007). A role played by crustal fluids is also inferred in the long lasting Pollino swarm (Napolitano et al. 2020; De Gori et al. 2022). The importance of stress transfer as triggering mechanism has also been documented in several cases (Brodsky and van der Elst 2014). Figure 7 shows the hypocenters obtained from the relative location, ordered by color from the first (blue) to the last (yellow), for the seven swarms analyzed in this paper. The error on the relative location is much smaller than the hypocenter distribution; therefore, a migration pattern would be meaningful. However, we do not observe any clear source migration with time. Therefore, we conclude that the occurrence of small seismic swarms and sequences at crustal depth in the Calabrian arc is due to a stress release in highly fractured volumes, not necessarily as part of large tectonic structures. The lack of any clear migration patterns suggests that the role of fluids and of stress transfer is negligible in the swarms analyzed in this work.

The daily number of earthquakes shows large differences among the analyzed swarms (Fig. 6). In three cases, Amantea, Catanzaro, and Umbriatico, the very most of events occurred during the first day, while for Albi and Mesima, the most of events occurred very scattered in time during about the first month.

A final remark regards the depth of analyzed earthquakes, which is higher than 10 km for six of the nine swarms resumed in Table 2. In three cases, Amantea, Catanzaro, and Umbriatico, all earthquakes are deeper than 20 km and reach the depth of 40 km for Catanzaro swarm. This means that these swarms cannot be reliably associated to any of the known seismogenic active faults. Thus, the study of small earthquake swarms is essential to identify and characterize active blind faults in the perspective of a better assessment of the seismic hazard.

Author contribution Giuseppe Davide Chiappetta performed most of data analysis, drew figures, and contributed to writing and interpretation. Mario La Rocca wrote the paper, contributed to data analysis, and interpreted the results.

Data availability Data used in this work comes from Università della Calabria (www.sismocal.org) and from Istituto Nazionale di Geofisica e Vulcanologia (www.ingv.it). Those not found in public databases (https://eida.ingv.it/it/) are available upon request to the authors.

Declarations

Competing interests The authors declare no competing interests.

References

Barani S, Ferretti G, Scafidi D, Spallarossa D (2014) Analysis of seismicity and micro-seismicity associated with the October–November 2010 Sampeyre swarm, Southwestern Alps. Tectonophysics 611(25):130–140. https://doi.org/10.1016/j.tecto.2013.11.017

Brodsky EE (2019) The importance of studying small earthquakes. Science 364(6442):736–737. https://doi.org/10.1126/science.aax2490

Brodsky EE, van der Elst NJ (2014) The uses of dynamic earthquake triggering. Annu Rev Earth Planet Sci 42:317–339. https://doi.org/10.1146/annurev-earth-060313-054648

Calderoni G, Gervasi A, La Rocca M, Ventura G (2021) Strike slip earthquakes at the northern edge of the Calabrian Arc subduction zone. Seismol Res Lett 92(2A):1023–1035. https://doi.org/10.1785/0220200251

Carmona E, Stich D, Ibañez JM, Saccorotti G (2009) Multiplet focal mechanisms from polarities and relative locations: the Iznajar Swarm in Southern Spain. Bull Seismol Soc Am 99(6):3421–3429. https://doi.org/10.1785/0120090036

Chen X, Shearer PM (2011) Comprehensive analysis of earthquake source spectra and swarms in the Salton Trough, California. J Geophysical Res: Solid Earth 116 (B9). https://doi.org/10.1029/2011JB008263

Chen X, Shearer PM, Abercrombie RE (2012) Spatial migration of earthquakes within seismic clusters in Southern California: Evidence for fluid diffusion. J Geophysical Res: Solid Earth 117 (B4). https://doi.org/10.1029/2011JB008973

De Gori P, Lucente FP, Govoni A, Margheriti L, Chiarabba C (2022) Seismic swarms in the Pollino seismic gap: Positive fault inversion within a popup structure. Front Earth Sci 10:968187. https://doi.org/10.3389/feart.2022.968187

Deichmann N, Garcia-Fernandez M (1992) Rupture geometry from high-precision relative hypocentre locations of microearthquake clusters. Geophys J Int 110(3):501–517. https://doi.org/10.1111/j.1365-246X.1992.tb02088.x

Ellsworth WL (2013) Injection-induced earthquakes. Science 341 (6142). https://doi.org/10.1126/science.1225942

Eyre TS, Eaton DW, Garagash DI, Zecevic M, Venieri M, Weir R, Lawton DC (2019) The role of aseismic slip in hydraulic fracturing–induced seismicity. Sci Adv 5 (8). https://doi.org/10.1126/sciadv.aav7172

Frepoli A, Amato A (2000) Fault plane solutions of crustal earthquakes in Southern Italy (1988–1995): seismotectonic implications. Ann Geofis 43(3):437–459

Giampiccolo E, Musumeci C, Falà F, Gresta S (2008) Seismological investigations in the Gioia Tauro basin (southern Calabria, Italy). Annal Geophysics 51(5–6). https://doi.org/10.4401/ag-3018

Got JL, Frechet J, Klein FW (1994) Deep fault plane geometry inferred from multiplet relative relocation beneath the south flank of Kilauea. J Geophys Res: Solid Earth 99(B8):15375–15386. https://doi.org/10.1029/94JB00577

Grasso JR, Amorese D, Karimov A (2021) Did wastewater disposal drive the longest seismic swarm triggered by fluid manipulations? Lacq. France Bull Seismol Soc Am 111(5):2733–2752. https://doi.org/10.1785/0120200359

Guerra I, Harabaglia P, Gervasi A, Rosa AB (2005) The 1998–1999 Pollino (Southern Apennines, Italy) seismic crisis: tomography of a sequence. Annals of Geophysics 48(6). https://doi.org/10.4401/ag-3249

Hainzl S, Fischer T, Dahm T (2012) Seismicity-based estimation of the driving fluid pressure in the case of swarm activity in Western Bohemia. Geophys J Int 191(1):271–281. https://doi.org/10.1111/j.1365-246X.2012.05610.x

Hainzl S, Ogata Y (2005) Detecting fluid signals in seismicity data through statistical earthquake modeling. J Geophys Res 110(B5). https://doi.org/10.1029/2004JB003247

Hauksson E, Andrews J, Plesch A, Shaw JH, Shelly DR (2016) The 2015 Fillmore earthquake swarm and possible crustal deformation mechanisms near the bottom of the Eastern Ventura Basin, California. Seismological Res Lett 87(4):807–815. https://doi.org/10.1785/0220160020

Hauksson E, Meier MA, Ross ZE, Jones LM (2017) Evolution of seismicity near the southernmost terminus of the San Andreas Fault: implications of recent earthquake clusters for earthquake risk in southern California. Geophys Res Lett 44(3):1293–1301. https://doi.org/10.1002/2016GL072026

Ito A (1985) High resolution relative hypocenters of similar earthquakes by cross-spectral analysis method. J Phys Earth 33(4):279–294. https://doi.org/10.4294/jpe1952.33.279

Jenatton L, Guiguet R, Thouvenot F, Daix N (2007) The 16,000-event 2003–2004 earthquake swarm in Ubaye (French Alps). J. G. R. 112(B11). https://doi.org/10.1029/2006JB004878

Kwiatek G, Martínez-Garzón P, Bohnhoff M (2016) HybridMT: a MATLAB/shell environment package for seismic moment tensor inversion and refinement. Seismological Res Lett 87(4). https://doi.org/10.1785/0220150251

Lohman RB, McGuire JJ (2007) Earthquake swarms driven by aseismic creep in the Salton Trough, California. J Geophysical Res: Solid Earth 112(B4). https://doi.org/10.1029/2006JB004596

McNutt SR (2005) Volcanic seismology. Annu Rev Earth Planet Sci 32:461–491. https://doi.org/10.1146/annurev.earth.33.092203.122459

Menke W (1984) Geophysical data analysis, discrete and inverse theory. Academic Press Inc. https://doi.org/10.1016/B978-0-12-490920-5.X5001-7

Michelini A, Margheriti L, Cattaneo M, Cecere G, D'Anna G, Delladio A, Moretti M, Pintore S, Amato A, Basili A, Bono A, Casale P, Danecek P, Demartin M, Faenza L, Lauciani V, Mandiello AG, Marchetti A, Marcocci C, Mazza S, Mele FM, Nardi A, Nostro C, Pignone M, Quintiliani M, Rao S, Scognamiglio L, Selvaggi G (2016) The Italian National Seismic Network and the earthquake and tsunami monitoring and surveillance systems. Adv Geosci 43(31–38):2016. https://doi.org/10.5194/adgeo-43-31-2016

Napolitano F, Gervasi A, La Rocca M, Guerra I, Scarpa R (2018) Site effects in the Pollino Region from the HVSR and polarization of seismic noise and earthquakes. Bull Seismol Soc Am 108(1):309–321. https://doi.org/10.1785/0120170197

Napolitano F, De Siena L, Gervasi A, Guerra I, Scarpa R, La Rocca M (2020) Scattering and absorption imaging of a highly fractured fluid-filled seismogenetic volume in a region of slow deformation. Geosci Front 11(3):989–998. https://doi.org/10.1016/j.gsf.2019.09.014

Napolitano F, Galluzzo D, Gervasi A, Scarpa R, La Rocca M (2021) Fault imaging at Mt Pollino (Italy) from relative location of microearthquakes. Geophys J Int 224(1):637–648. https://doi.org/10.1093/gji/ggaa407

Orecchio B, Neri G, Presti D, Scolaro S, Totaro C (2021) Seismic deformation styles in the upper and lower plate domains of the Calabrian subduction zone, south Italy.

J Geodynamics 145. https://doi.org/10.1016/j.jog.2021.101847

Parotidis M, Shapiro SA, Rothert E (2005) Evidence for triggering of the Vogtland swarms 2000 by pore pressure diffusion. J Geophys Res 110(B5). https://doi.org/10.1029/2004JB003267

Passarelli L, Rivalta E, Jónsson S, Hensch M, Metzger S, Jakobsdóttir SS, Maccaferri F, Corbi F, Dahm T (2018) Scaling and spatial complementarity of tectonic earthquake swarms. Earth Planet Sci Lett 482:62–70. https://doi.org/10.1016/j.epsl.2017.10.052

Pastori M, Margheriti L, De Gori P, Govoni A, Lucente FP, Moretti M, Marchetti A, Di Giovambattista R, Anselmi M, De Luca P, Nardi A, Agostinetti NP, Latorre D, Piccinini D, Passarelli L, Chiarabba C (2021) The 2011–2014 Pollino Seismic Swarm: Complex Fault Systems Imaged by 1D Refined Location and Shear Wave Splitting Analysis at the Apennines–Calabrian Arc Boundary. Front Earth Sci 9. https://doi.org/10.3389/feart.2021.618293

Pino NA, Piatanesi A, Valensise G, Boschi E (2009) The 28 December 1908 Messina Straits Earthquake (Mw 7.1): A Great Earthquake throughout a Century of Seismology. Seism Res Lett 80(2):243–259. https://doi.org/10.1785/gssrl.80.2.243

Presti D, Billi A, Orecchio B, Totaro C, Faccenna C, Neri G (2013) Earthquake focal mechanisms, seismogenic stress, and seismotectonics of the Calabrian Arc, Italy. Tectonophysics 602:153–175. https://doi.org/10.1016/j.tecto.2013.01.030

Roland E, McGuire JJ (2009) Earthquake swarms on transform faults. Geophys J Int 178(3):1677–1690. https://doi.org/10.1111/j.1365-246X.2009.04214.x

Ross Z, Trugman DT, Hauksson E, Shearer PM (2019) Searching for hidden earthquakes in Southern California. Science 364(6442):767–771. https://doi.org/10.1126/science.aaw6888

Ross ZE, Cochran ES (2021) Evidence for latent crustal fluid injection transients in Southern California from long-duration earthquake swarms. Geophysical Res Lett 48(12). https://doi.org/10.1029/2021GL092465

Rovida A, Locati M, Camassi R, Lolli B, Gasperini P (2020) The Italian earthquake catalogue CPTI15. Bull Earthq Eng 18:2953–2984. https://doi.org/10.1007/s10518-020-00818-y

Rovida A, Locati M, Camassi R, Lolli B, Gasperini P, Antonucci A (2022) Catalogo Parametrico dei Terremoti Italiani (CPTI15), versione 4.0. Istituto Nazionale di Geofisica e Vulcanologia (INGV). https://doi.org/10.13127/CPTI/CPTI15.4

Scherbaum F, Wendler J (1986) Cross spectral analysis of Swabian Jura (SW Germany) three-component microearthquake recordings. J Geophys 60(1):157–166

Schweitzer J (2001) HYPOSAT - an enhanced routine to locate seismic events, Pure appl. Geophys 158:277–289. https://doi.org/10.1007/PL00001160

Schweitzer J (2006) How can the ISC location procedures be improved? Phys Earth Planet Inter 158(1):19–26. https://doi.org/10.1016/j.pepi.2006.03.017

Shearer PM, Hardebeck JL, Astiz L, Richards-Dinger KB (2003) Analysis of similar event clusters in aftershocks of the 1994 Northridge earthquake. J Geophysical Res: Solid Earth 108(B1). https://doi.org/10.1029/2001JB000685

Snoke JA, Munsey JW, Teague AG, Bollinger GA (1984) A program for focal mechanism determination by combined use of polarity and SV-P amplitude ratio data. Earthquake Notes 55(3):15

Stich D, Alguacil G, Morales J (2001) The relative locations of multiplets in the vicinity of the Western Almeria (southern Spain) earthquake series 1993–1994. Geophys J Int 146(3):801–812. https://doi.org/10.1046/j.0956-540x.2001.01498.x

Suarez G, Sanchez-Alvaro E, Lomas-Delgado E, Arvizu-Lara G (2016) The 2013 seismic swarm in Chihuahua, Mexico: evidence of active extensional deformation in the southern Basin and Range. Bull Seism Soc Am 106(6):2686–2694. https://doi.org/10.1785/0120160179

Tertulliani A, Cucci L (2009) Clues to the identification of a seismogenic source from environmental effects: the case of the 1905 Calabria (Southern Italy) earthquake. Nat Hazards Earth Syst Sci 9:1787–1803. https://doi.org/10.5194/nhess-9-1787-2009

Thouvenot F, Jenatton L, Scafidi D, Turino C, Potin B, Ferretti G (2016) Encore Ubaye: earthquake swarms, foreshocks, and aftershocks in the Southern French Alps. Bull Seism Soc Am 106(5):2244–2257. https://doi.org/10.1785/0120150249

Totaro C, Presti D, Billi A, Gervasi A, Orecchio B, Guerra I, Neri G (2013) The ongoing seismic sequence at the Pollino Mountains. Italy Seismological Res Lett 84(6):955–962. https://doi.org/10.1785/0220120194

Totaro C, Seeber L, Waldhauser F, Steckler M, Gervasi A, Guerra I, Orecchio B, Presti D (2015) An intense earthquake swarm in the southernmost Apennines: fault architecture from high-resolution hypocenters and focal mechanisms. Bull Seismol Soc Am 105(6):3121–3128. https://doi.org/10.1785/0120150074

Van Noten K, Lecocq T, Shah AK, Camelbeeck T (2015) Seismotectonic significance of the 2008–2010 Walloon Brabant seismic swarm in the Brabant Massif, Belgium. Tectonophysics 656:20–38. https://doi.org/10.1016/j.tecto.2015.05.026

Vidale JE, Shearer PM (2006) A survey of 71 earthquake bursts across southern California: exploring the role of pore fluid pressure fluctuations and aseismic slip as drivers. J Geophys Res 111(B5). https://doi.org/10.1029/2005JB004034

Zhu L, Ben-Zion Y (2013) Parametrization of general seismic potency and moment tensors for source inversion of seismic waveform data. Geophys J Int 194(2):839–843. https://doi.org/10.1093/gji/ggt137